Magnetic capture of individual biological cells and model aggregates of cell membranes

A. M. Shalygin and K. A. Krotov

M. V. Lomonosov State University, Moscow

Usp. Fiz. Nauk **160**, 83–104 (July 1990)

Studies are reviewed on the development and application of a new method of measuring the magnetic susceptibility of single biological cells and liposomal bilayer aggregates that model the core of the cell membrane, and also any nonmagnetic and weakly magnetic microparticles of volume of the order of 10^{-10} cm^3, without violating their integrity. The method is based on the phenomenon of magnetophoretic motion of cells in a buffer medium caused by the interaction of the magnetic moment of the cell induced by an external magnetic field with the fringing field of a thin magnetic filament magnetized by the same field. It enables measuring induced moments of either sign of the order of $10^4 - 10^5$ Bohr magnetons in a field of 1 kOe. The potentialities of the method are illustrated by the results of studies of the magnetic properties of human erythrocytes containing hemoglobin in the fundamental forms obtained as functions of the temperature, the pH of the medium, and oxygen-exchange processes. The properties of hemoglobin in cells and solutions are compared. The possibility is noted of identifying the magnetic properties and the physiological state of the cells. By using magnetic capture of spherical and cylindrical multilayer liposomes, one can obtain the most complete information on the magnetic properties of the lipid bilayer–its magnetic susceptibility, diamagnetic anisotropy, and the components of the magnetic susceptibility tensor. These potentialities of magnetic capture have been realized experimentally, and by using it new information has been obtained on the features of the thermotropic behavior of membrane bilayers of synthetic dipalmitoyllecithin in the region of the fundamental phase transition and of bilayers of natural phospholipids–egg lecithin and the total lipids of erythrocyte membranes in the region of thermal structural rearrangements. The high sensitivity of magnetic capture to a change of the state of the lipid bilayer and its information content with respect to structural organization are noted.

INTRODUCTION

The study of the individual magnetic properties of functioning biological cells, cell fragments, and organelles, as well as model analogs of them, such as bilayer aggregates of lyotropic mesophases, appears to be of great importance and interest.[1,2] This interest arises from the natural tendency to expand the field of physical studies to a known nonequilibrium object whose state is determined in many ways, not only by such parameters as the temperature and pressure, but also by the composition and state necessary for its functioning in the surrounding buffer medium. A condition of no small importance for advancing along this line is the choice or artificial creation of a very simple object, knowing how to measure its properties, in particular, also its magnetic properties, without violating the integrity of the object and its inner bonding. We can add that an understanding of the leading and intensively developing studies on the influence of magnetic fields on cells, tissues, and organisms is impossible without knowing the material constants of the molecular and supermolecular structures of the cell, in particular, their static and dynamic magnetic susceptibilities.[3]

The known methods of experimental study of the magnetic properties of matter, such as the Faraday magnetic balance or the recently developed supersensitive SQUID magnetometry cannot be used for measurements of such small magnetic moments as the moment induced by an external magnetic field in an individual isolated nonmagnetic microparticle of volume 10^{-10} cm^3, such as a biological cell. Studies of the magnetic properties of microobjects make a number of demands on the technique and methodology of the measurements. Thus, the object of study requires a definite environment to maintain its functional state and the corresponding manifestation of its specific properties–a buffer medium whose magnetic susceptibility is close to that of the object itself. Moreover, often one must distinguish the contribution from some part of the object that constitutes several percent of its mass or volume.

The extremely high sensitivity sufficient to measure the magnetic susceptibility of single cells with an induced magnetic moment of either sign relative to the medium of the order of $10^4 - 10^5$ Bohr magnetons in a 1-kOe field[1)] is possessed by a technique that uses strongly inhomogeneous fringing fields arising near the surface of a thin magnetic filament when it has been transversely magnetized. These experiments study the parameters of motion of the cell caused by the interaction of the magnetic moment of the cell induced by the external field with the fringing field of the magnetic filament magnetized by the same field (Fig. 1a). Here the essential factors are the magnitude and sign of the difference $\chi = \chi_p - \chi_{buf}$ between the magnetic susceptibilities of the particle χ_p and of the buffer medium χ_{buf}. Thus, for particles with $\chi > 0$ one observes the phenomenon of

 0038-5670/90/070541-13$01.00

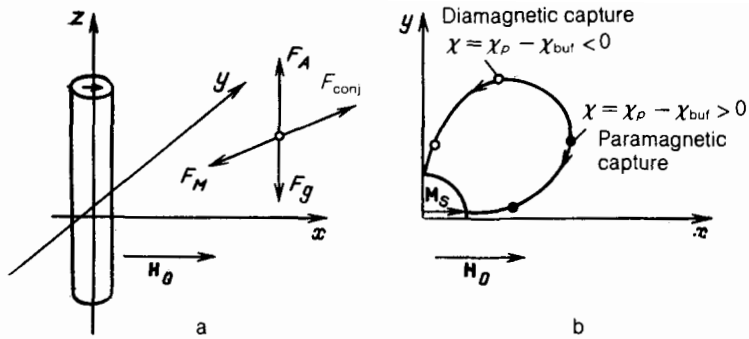

FIG. 1. Schematic drawing of a filament and a particle in a magnetic-capture experiment (a); projections of the trajectories of motion of particles in the xy plane in diamagnetic and paramagnetic capture (b).

paramagnetic capture–attraction of the particles into the region of greatest field intensity near the surface of the filament, while for particles with $\chi < 0$ one observes diamagnetic capture–attraction of particles (more diamagnetic than the medium) into the region of least field intensity at the surface of the filament (Fig. 1b). The high sensitivity in these measurements arises from the considerable increase in the product H grad H owing to the use of thin filaments whose diameters are comparable with the diameter of the cells or particles being studied, as well as the compensative character of the measurements: magnetic capture is the only compensative method among the magnetic measurements known in practice; the susceptibility of the object here is determined relative to the susceptibility of the buffer medium, which is assumed to have been already determined, and as a rule, is of the same or similar order of magnitude as that of the particle being studied.

1. EXPERIMENTAL SCHEME. CALCULATED RELATIONSHIPS

An experimental scheme for magnetic capture of cells is shown in Fig. 1a, from which we see that the projections of the trajectories of the particles of interest to us lie in the xy plane perpendicular to the axis of the filament and to the force of gravity. The motion of a particle in this plane is governed by the action of the ponderomotive force, which is balanced (upon neglecting the inertial contribution) by the force of resistance, which can be represented by the Stokes formula at low velocities of motion of the cells.

The equations of motion of a homogeneous spherical particle of radius R ($R \ll a$, where a is the radius of the filament) in the coordinates r, φ with account taken of the magnetic potentials satisfying the Laplace equation have the form[4,5]

$$\dot{r}_a = \frac{V_M}{a}\left(\frac{k}{r_a^5} + \frac{\cos 2\varphi}{r_a^3}\right),$$
$$r_a\dot{\varphi} = \frac{V_M}{a}\frac{\sin 2\varphi}{r_a^5}, \tag{1}$$

Here we have $r_a = r/a$, $V_M = \chi V M_s H_0/6\pi\eta a R_{eff}$, $k = M_s/2H_0$, M_s is the saturation induction of the filament material, η is the viscosity of the buffer, V is the volume of the particle, H_0 is the intensity of the external magnetic field, and R_{eff} is the effective hydrodynamic radius of the particle.

The family of trajectories is obtained (Fig. 2) by integrating the system of Eqs. (1):

$$r_a^2 = c \sin 2(\varphi - \alpha), \tag{2}$$

Here we have

$$c = (r_{a1}^4 + 2kr_{a1}^2 \cos 2\varphi_1 + k^2)^{1/2} (\sin 2\varphi_1)^{-1},$$
$$\operatorname{tg} 2\alpha = \frac{k \sin 2\varphi_1}{r_{a1}^2 + k \cos 2\varphi_1}, \quad \sin 2\varphi_1 \neq 0;$$

Here r_{ai} and φ_i are the initial coordinates of the particle. When $\sin 2\varphi_1 = 0$, the particle moves along one of the "straight" trajectories–along one of the axes x or y. The form of the trajectories and the character of the magnetic capture are determined by the value of the parameter $k = M_s/2H_0$. Figure 2 shows the families of trajectories for $k = 1$ and $k = 0$. As we see, the character of the trajectories of the two limiting cases strongly differs–when $k = 1$ the family diverges from the single point $\pi/2$, while when $k = 0$ it lies symmetrically with respect to π/r. Let $k = 1$, i.e., the field H_0 is weak, though magnetizing the filament to saturation. Then the region of diamagnetic capture at the surface of the filament to which particles with $\chi < 0$ are attracted degenerates into a line along the generator corresponding to $\varphi = \pi/2$. Here almost the entire surface expands. In an extremely strong field it tends to become comparable with the zone of paramagnetic capture ($k = 0$).[2)]

The separation of the space around the filament into regions of magnetic capture of opposite signs is determined by the values of the critical angles φ_{cr}

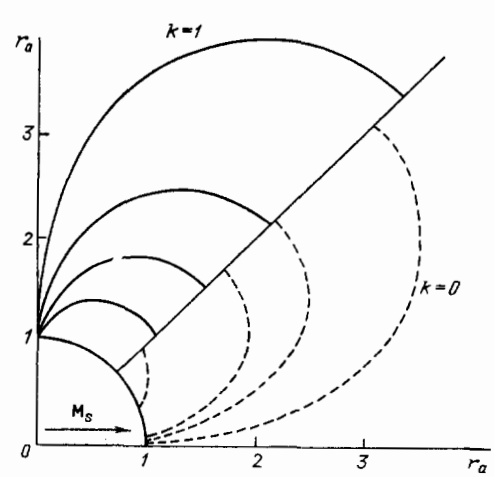

FIG. 2. Families of magnetic-capture trajectories of point particles for the cases $k = 1$ (a) and $k = 0$ (b).

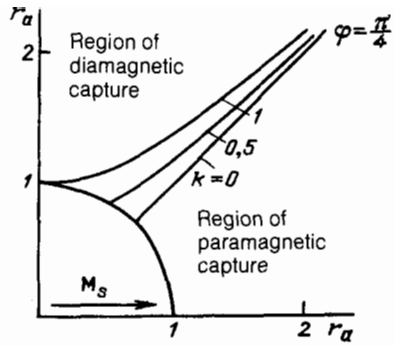

FIG. 3. Dependence of the critical angles φ_{cr} (r_a) for different values of the parameter $k = M_s/2H_0$.[7]

$$F_{Mr} = -\frac{\chi V M_s a^2}{r^3}\left(H_0 \cos 2\varphi + \frac{M_s a^2}{2r^3}\right), \qquad (3)$$
$$F_{M\varphi} = \chi V M_s a^2 H_0 \sin 2\varphi r^{-3}$$

Here the radial component of the force acting on the particle changes sign, i.e., we have

$$\varphi_{\text{кр}} = \operatorname{arctg}\left[\frac{1+(k/r_a^2)}{1-(k/r_a^2)}\right]^{1/2}. \qquad (4)$$

Figure 3 shows the φ_{cr} (r_a) relationship for different values of k.[7] In the region $0<\varphi<\varphi_{cr}$ we should expect attraction of particles with $\chi>0$ and repulsion of those with $\chi<0$, while conversely,in the region $\varphi_{cr}<\varphi<\pi/2$ we expect attraction with $\chi<0$ and repulsion with $\chi>0$.

The expression for χ is obtained by integrating (1) along the trajectory over the interval $[r_{a1},\varphi_1;r_{a2},\varphi_2]$; r_{a2} and φ_2 are the final coordinates of the particle:

$$\chi = \frac{3\pi\eta R_{\text{eff}} a^2}{H_0 M_s V}\,\frac{F(r_{a1}, r_{a2}, \varphi_1, \varphi_2, k)}{t}, \qquad (5)$$

Here t is the time of passage of the particle along the stated segment of the trajectory ($t<0$), while we have

$$F(r_{a1}, r_{a2}, \varphi_1, \varphi_2, k) = 2c^2\Big[\sin(\varphi_1+\varphi_2-4\alpha) \times \sin(\varphi_1-\varphi_2) + \frac{1}{2}\sin^2 2\alpha \cdot \ln\frac{\operatorname{tg}\varphi_1}{\operatorname{tg}\varphi_2}\Big] \qquad (6)$$

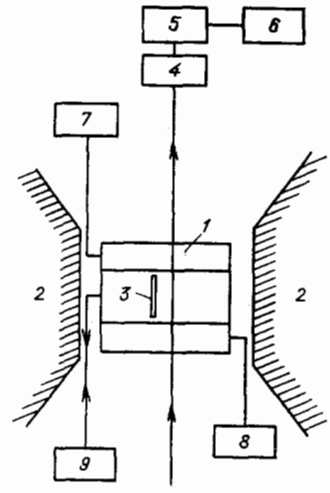

FIG. 4. Diagram of the experimental setup for observing and measuring magnetic-capture trajectories. *1*–thermostatted cuvette; *2*–pole pieces of the electromagnet; *3*–thin magnetic filament; *4*–videocamera; *5*–videorecorder; *6*–telemonitor; *7*–thermostat; *8*–thermocouple; *9*–peristaltic pump.

when $\sin 2\varphi_1 \neq 0$ and for "straight" trajectories, i.e., when $\sin 2\varphi_1 = 0$, we have

$$F(r_{a1}, r_{a2}, k) = \mp\frac{1}{2}(r_{a1}^4 - r_{a2}^4) \mp k(r_{a1}^2 - r_{a2}^2) + k^2 \ln\frac{k \pm r_{a1}^2}{k \pm r_{a2}^2}. \qquad (7)$$

2. MAGNETIC CAPTURE OF CELLS

The family of trajectories of (2) and the calculational relationships of (5) were derived for a particle with $R \ll a$ in the approximation in which a nonviscous flux flows around it. The possibilities of using them for defining cells were studied mainly with red blood cells–human erythrocytes. Erythrocytes are easily accessible non-nucleated blood cells[8] of discoidal type, of diameter $\sim 8\,\mu$m, homogeneous in composition (they contain $\sim 71\%$ water and $\sim 28\%$ hemoglobin (Hb). What is of no small importance is that they can have a susceptibility relative to the buffer differing in magni-

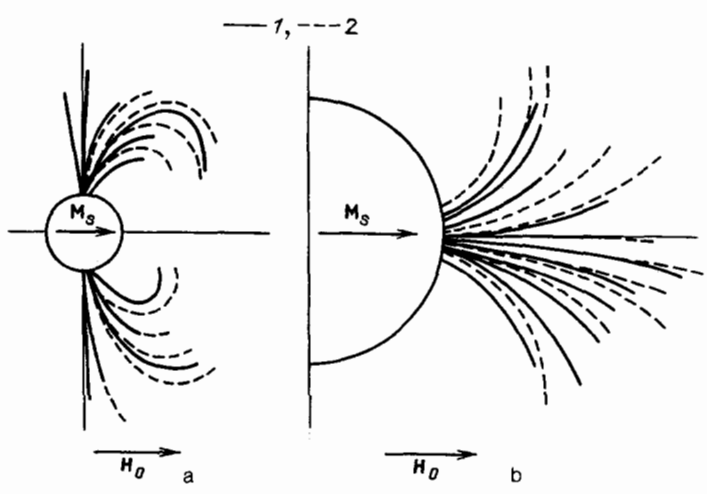

FIG. 5. Experimental (*1*) and calculated (*2*) trajectories of cells in diamagnetic capture ($a = 10\,\mu$m, $k = 0.18$) (a), and in paramagnetic capture ($a = 55\,\mu$m, $k = 0.23$) (b).[14]

tude and sign[9,10] by an order of magnitude, which is unambiguously determined by the state of the hemoglobin contained in them. In the case of its fundamental forms, this can easily be monitored spectrophotometrically.

The observation and measurement of the parameters of the trajectories of motion of cells near the surface of a transversely magnetized filament in the case of magnetic capture are performed in air-tight cuvettes several tenths of a mL in volume (see, e.g., Refs. 11, 12, 13). The cuvette with the filament fixed in it is placed on the specimen stage of a microscope between the pole pieces of an electromagnet so as to bring about the arrangement of the filament, the particle, and direction of the magnetizing field H_0 indicated in Fig. 1.[3)]

An illumination ray propagating along the axis of the filament (Fig. 4) transmits an image of the cross section of the filament and of the cells lying in the field of view of the microscope to the vidicon of a videocamera connected to a video tape recorder. The motion of the cells in magnetic capture is determined by video recording, the processing of which enables one to determine the initial and final coordinates of a particle and its time of motion between them. Fig. 5 shows typical trajectories of the diamagnetic capture of erythrocytes containing $\sim 99\%$ oxyhemoglobin and the paramagnetic capture of erythrocytes containing deoxy- and methemoglobin.[14] The dashed lines there show the trajectories calculated by (2) and adjusted to experiment with account taken of the actual experimental parameters. As we see from the diagram, the best agreement is observed for cells moving in capture along "straight lines" or trajectories close to them.

As Eq. (5) implies, the ratio F/t, apart from a constant coefficient, determines the magnetic susceptibility of the particle with respect to the medium. The magnitude of this coefficient depends on the ratio R_{eff}/V, which for cells is an effective value owing to local distortions of shape, the presence of a surface charge and ion shell, and also owing to the nonabsolute elasticity and smoothness of the cell membrane, which are manifested in its motion in a liquid.As regards erythrocytes, their defect as model cellular particles is the absence of spherical symmetry of the cell shape and their extreme elasticity, which affects the accuracy of determining R_{eff}/V. However, in view of the discoidal shape, in sedimentation and magnetic capture in a highly dilute suspension, an erythrocyte moves in the plane of its disk. The determination of the ratio R_{eff}/V is usually performed in separate experiments, e.g., in settling of the cells in the gravity force field. Thus, apart from the ratio R_{eff}/V, the distribution of the cells with respect to F/t corresponds to their distribution with respect to magnetic susceptibility. The ratio F/t of a cell is determined as follows. The magnetic-capture trajectory of the particle is divided into segments. For each segment one determines the coordinates of the start and the end and the time of passage of the particle through it, whereupon one constructs the $F/(t)$ relationship. Figure 6 shows a typical form of such relationships obtained in the magnetic capture of erythrocytes containing hemoglobin in the fundamental forms, and also of human lymphocytes as they move along "straight lines" or trajectories close to them. As we see from the diagram, F varies linearly with the time, which agrees with (5) and which enables one to use this circumstance to determine the χ of the cells.

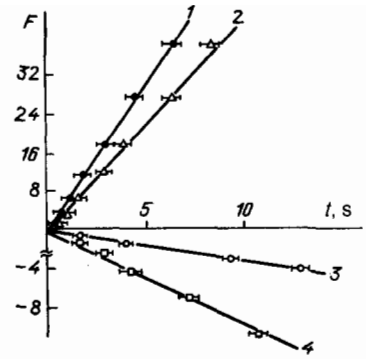

FIG. 6. Examples of $F(t)$ dependences for erythrocytes containing methemoglobin (*1*), deoxyhemoglobin (*2*), and oxyhemoglobin (*3*), and human lymphocytes (*4*).[13]

A deviation from a linear $F(t)$ relationship is observed either far from the filament for large radii of capture, where it arises from the uncertainty in establishing the time of passage of the cell through remote segments of the trajectories,[13] or in the immediate vicinity of the filament,[11,12] owing to hindrance caused by the incompressibility of the liquid. In the latter case, owing to the Stokes resistance, one can introduce a correcting parameter λ,[15] which "compensates" the hindering action of the wall (Fig. 7):

$$\lambda = \frac{4}{3}\operatorname{sh}\alpha \sum_{n=1}^{\infty} \frac{n(n+1)}{(2n-1)(2n-3)} \times \left\{ \frac{2\operatorname{sh}(2n+1)\alpha + (2n+1)\operatorname{sh}2\alpha}{4\operatorname{sh}^2[n+(1/2)]\alpha - (2n+1)\operatorname{sh}^2\alpha} - 1 \right\},$$

$$\alpha = \operatorname{arcch}\frac{r-a}{R}. \tag{8}$$

Deviations from a linear $F(t)$ dependence were also noted for cells for which one observed a poorer adjustment of the calculated trajectories to those experimentally observed (see Fig. 5), i.e., for cells moving along "curved" trajectories. Here, the greater the deviation,the more curved was the trajectory of cell motion. Perhaps both circumstances involve the need of taking account of the viscous corrections and the finite dimensions of the cells, which are manifested in their motion along "curved" trajectories.

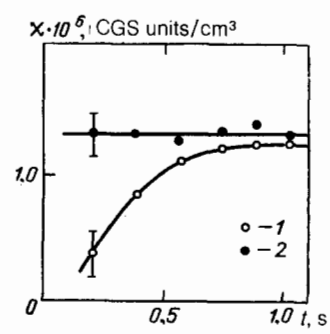

FIG. 7. Relative magnetic susceptibility of an erythrocyte as a function of its distance from the filament (measured at different instants of time of magnetic capture) as calculated from capture data without taking account (*1*) and with taking account (*2*) of the hindering action of the surface of the filament.[12]

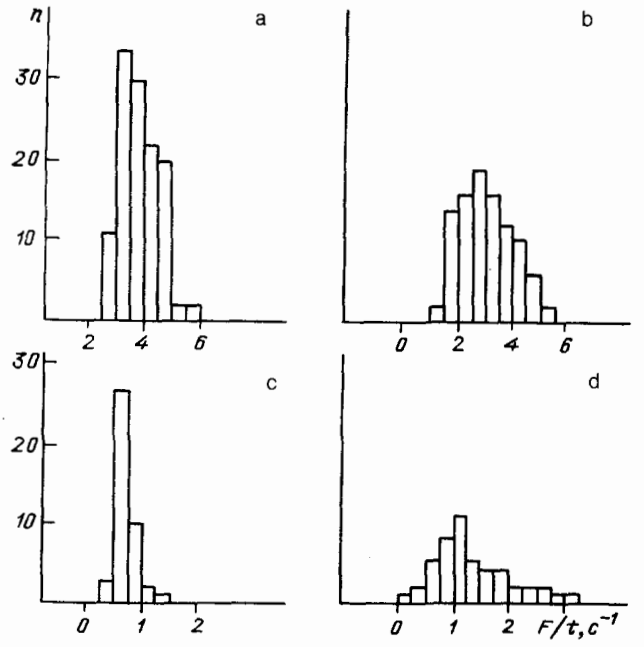

FIG. 8. Typical histograms of the value of $F(t)$ of erythrocytes containing methemoglobin (a), deoxyhemoglobin (b), oxyhemoglobin (c), and of lymphocytes (d).[13]

Taking account of the finite dimensions of particles having the form of a disk and moving along straight trajectories leads to insignificant corrections, which are manifested at the surface of the filament and for particles with $R = 5$ μm for filaments with diameter 20 μm, and which proves to be smaller than the error of measurement of the capture parameters.[13]

Analysis of the trajectories of erythrocytes in capture showed[13] that cells that pass through one particular point in the $r\varphi$ coordinate plane move further, until the moment of capture, along the same trajectory, regardless of the magnetic susceptibility of the cell. This allows us to assume that the difference in time of passage of cells of similar dimensions through the same segment of trajectory arises from their differing values of the magnetic susceptibility.

The magnetic susceptibility of a group of cells under study is determined by using the probable values of their sedimentation velocities and magnitudes of F/t as determined from the corresponding histograms obtained from the data of observations of "straight" or near-straight trajectories of the magnetic capture of the cells. Examples of histograms of the value of F/t of erythrocytes containing hemoglobin in the fundamental forms are shown in Fig. 8.[13] The position of the maxima of the histograms and their form reflects the homogeneity of composition of each studied group of erythrocytes and enables one to determine the value of their mean magnetic susceptibility. The value of F/t is highly sensitive to the content in the cells of various impurities. Thus, for conditions the same as in Fig. 8, the difference between the calculated time of passage of an idealized cell containing all its hemoglobin in the oxy form to the same cell with an admixture of 0.5% methemoglobin[4)] through the same segment of trajectory equal to the diameter of the cell amounts to ~ 2.5 s during capture.[17] The same diagram shows the histogram of the F/t distribution of human lymphocytes, which confirms the extremely broad spectrum of magnetic properties of these cells.[18] In studying cells having a small induced magnetic moment, e.g., oxygenated erythrocytes or freshly isolated human lymphocytes, one must achieve the highest sensitivity with respect to magnetic moment. The magnitude of grad H, which determines the force acting on the particle, is limited by the curvature of the source of the gradient field, which must exceed somewhat the dimensions of the cell under study so that its drift during capture should amount to at least several of its diameters (usually 3–5), as is necessary to measure F/t. Thus the sensitivity with respect to magnetic moment for a fixed saturation induction of the material of the filament, whose diameter is chosen on the basis of the dimensions of the cell, is determined only by the magnitude of the external magnetic field. The smallest measured value of the magnetic moment amounted to $\sim 10^5$ Bohr magnetons in a field of 1 kOe for oxygenated human erythrocytes.[14]

When one must make multiple measurements of the magnetic capture of the same cell, one should use a somewhat different mutual arrangement of the filament with respect to the direction of the magnetizing field and to the force of gravity. The scheme of such an experiment will also differ in the orientation of the magnetizing field with respect to the direction of the force of gravity for cells having the opposite sign of the susceptibility relative to the buffer (Fig. 9). Since the density of the cells slightly exceeds that of the buffer (the density of erythrocytes is 1.096 g/cm^3), then for the schemes shown in Fig. 9 and cells with either sign of χ, by manipulating the turning on and off of the magnetic field (without allowing the cell to be captured), one can center its motion along the vertical axis. Then one can perform multiple measurements of the vertical displacements of the chosen cell upon capture by measuring the capture parameters with the field turned on, and the value of the effective hydrodynamic radius with the field turned off. Here one must introduce into the equation of motion of the particle the force of gravity, which has the result that the expressions for χ of the cell will not have an analytic form and will be determined by simple numerical calculations that also depend on the initial and final coordinates of the cell in capture and the time of passage between them.

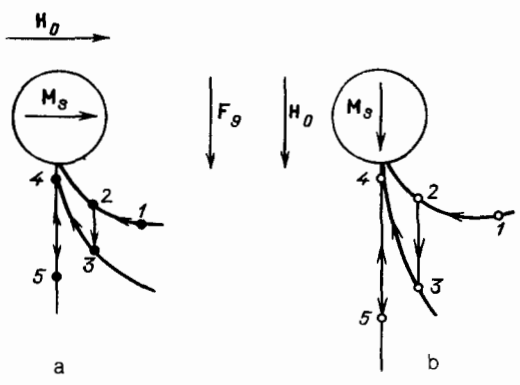

FIG. 9. Mutual arrangement of the filament, the particle, and the direction of the magnetizing field H_0 in an experiment on magnetic capture that enables performing multiple measurements of the magnetic capture of an individual cell with diamagnetic (a) and paramagnetic (b) susceptibility with respect to the buffer medium.

3. THE MAGNETIC SUSCEPTIBILITY OF HUMAN ERYTHROCYTES

In studies of magnetic capture, which are the basis of high-gradient magnetic separation,[19,20] one can note several points in the use of erythrocytes as model cell systems:

–for studying the possibility of magnetic separation of biological cells by using high-gradient magnetic filters,[21-23]

–for experimental verification of the concepts of high-gradient magnetic separation under development,[24]

–for developing these concepts in the special case of an established flux as a method of measuring the magnetic susceptibility of biological cells,[10,11] and finally

–for studying the magnetic properties of specific single cells without violating their integrity and conditions of functioning. We shall illustrate the latter with examples of studies of the magnetic properties of human erythrocytes that we have conducted.

Erythrocytes are considered to be relatively simple cells. Their fundamental function is to transport oxygen to the tissues of the organism, which they fulfill with the use of hemoglobin.[5)] The active centers of the Hb molecules are four iron atoms, which make possible the cooperative character of the binding of Hb with oxygen. In the stereochemical model of hemoglobin[26] the basis of the cooperative binding of Hb with oxygen is the intercoupling of the quaternary structure of the protein and the spin state of the heme iron. Magnetic susceptibility has always served as a means of studying the properties of hemoglobins in solution. Therefore studies of the magnetic properties of individual erythrocytes, and of hemoglobin and its derivatives contained in them, whose state arises from the spin state of the iron, and its change upon ligand exchange, as well as the change in the conditions of functioning of the protein, are both of independent interest and of interest in comparison with the properties of hemoglobin solutions.

3.1. Magnetic susceptibility of intracellular oxyhemoglobin

Measurements of the magnetic susceptibility of solutions of hemoglobin[27] have shown that oxyhemoglobin (oxyHb) is diamagnetic and the effective moment of the complex of heme iron with oxygen equals zero. There are several models[28-30] that explain the diamagnetism of HbO_2. Some preference is granted to the model of Ref. 30, in which the reversible oxygen binding occurs by the scheme

$$\underset{\text{deoxyHb}}{\mathrm{Hb}(\mathrm{Heme}\ d_2^6)} + O_2 \rightleftarrows \underset{\text{oxyHb}}{\mathrm{Hb}(\mathrm{Heme}\ d_{1/2}^5)\,O \cdot O^-}, \qquad (9)$$

which presupposes charge transport in HbO_2 from the iron ion Fe^{2+} to the molecule of oxygen to form the ionic bound complex ($Fe^{3+}\,O_2^-$). The absence of magnetism here is explained by the existence of antiferromagnetic coupling between the spins of the metal and the ligand. The concepts that have ben developed were cast into doubt by a study[31] performed with a SQUID magnetometer, which found the existence of paramagnetism of oxyHb. These measurements did not agree with the earlier measurements of the magnetic susceptibility of oxygenated erythrocytes performed by the method of magnetic capture.[9] Later it turned out that they were due to methodological error that arose in developing the method of measuring the magnetic susceptibility of Hb solutions using SQUID magnetometry and were corrected, both by studies of the authors themselves[32] and of other investigators.[33,34] Nevertheless, the revealed instability of oxyHb as a final state, especially the instability of its natural forms in erythrocytes,[35] required a refinement of the magnitudes of its magnetic susceptibility as a function of the temperature and of the properties of the surrounding medium.

The study of the magnetic susceptibility of intracellular hemoglobin was performed on individual cells in a dilute suspension by the magnetic-capture method in the temperature interval 2–55 °C and with variation of the pH of the buffer medium from 4.5 to 9.5. Figure 10 shows the temperature dependence of the ratio F/t, which is proportional to the magnetic susceptibility of the cells. Each point is a mean value obtained from the histogram of the distribution with respect to values of F/t of 50–100 cells of similar dimension. We see that the dependence is nonmonotonic in character with weakly marked features in the temperature regions 7–12, 20–25, and 35–37 °C. At ~42.5 °C a sign change occurs in the magnetic capture. The magnetic susceptibility of the cells becomes more "paramagnetic" than the susceptibility of the medium, and their motion converts from the diamagnetic to the paramagnetic mode. As was noted, the ratio F/t corresponds, apart from R_{eff}/V, to the magnetic susceptibility of the cell. If we assume that the erythrocyte contains a solution of hemoglobin with the concentration c_c^{Hb}, we see from the relationship

$$6\pi v_s \eta R_{\mathrm{eff}} = g\,(\rho_{\mathrm{Hb}} - \rho_{\text{буф}})c_c^{\mathrm{Hb}} \qquad (10)$$

with an invariant amount of intracellular hemoglobin, i.e., $c_c^{\mathrm{Hb}} \cdot V$, that the value of $1/v_s\eta$, where v_s is the sedimentation velocity of the cell, is proportional to R_{eff}. Figure 11 shows the temperature dependence of $1/v_s\eta$ of the same dilute cell suspension. We also see in this dependence features of the sedimentation of the erythrocytes in the regions 7–12, 20–25, and 35–37 °C that are correlated with their magnetic-capture features: the magnetic susceptibility of intracellular Hb relative to the buffer (Fig. 12) as constructed by (5) from the data of Figs. 10 and 11 now has a monotonic temperature trend. Apparently the features observed in the temperature dependences of $1/(v_s\eta)$ and F/t are due to features of the thermotropic properties of the erythrocyte membranes[36] that lead to changes in the R_{eff} of the cells. However, without taking up a discussion of these features, we note the sensitivity of magnetic capture to them, which proves essential in studying model analogs of biological membranes (see below).

As it turned out, the magnetic susceptibility of intracellular Hb is practically independent of the temperature in the

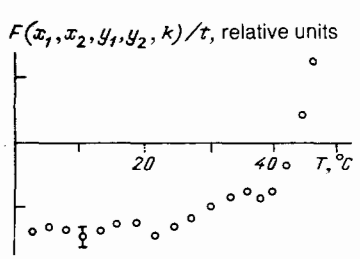

FIG. 10. Temperature dependence of the rate of magnetic capture F/r of oxygenated erythrocytes (pH ~ 7.4).

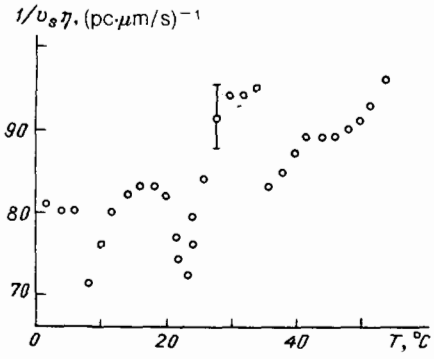

FIG. 11. Temperature dependence of $1/(\eta v_s)$ of erythrocytes sedimenting in a buffer (pH ~ 7.4).

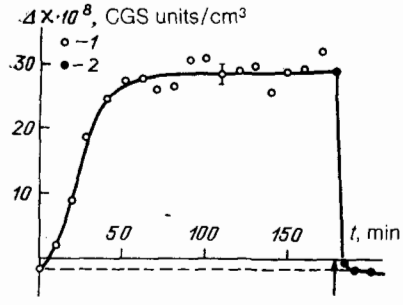

FIG. 13. Susceptibility of individual erythrocytes with respect to the buffer (25 °C, pH ~ 7.4) as a function of the time of diffusion of oxygen through a gas-permeable membrane. *1*–diffusion of oxygen from the suspension upon blowing argon at the cell; *2*–diffusion into the deoxygenated suspension upon blowing air at the cell.

range 2–30 °C and amounts to $\chi = -(0.774 \pm 0.005) \times 10^{-6}$ CGS units/cm^3. Similar results have been obtained also by other authors, both in studying cells[35,37] and solutions.[33,34] Above 35 °C one observes a sharp increase in the susceptibility of Hb (see Fig. 12).[38] Measurements performed after bubbling the suspension with oxygen for 30 min at 45 °C showed that the increase in susceptibility is caused by a change in the partial pressure of dissolved oxygen with increasing temperature and thermal deoxygenation of Hb, which leads to a shift in equilibrium of the combination of oxygen with Hb toward the original reagents. The reversibility of the susceptibility upon repeated variations of temperature from 20 to 40 °C characterizes the thermal deoxygenation, while the presence of hysteresis indicates methemoglobinization, i.e., irreversibility of the oxidation of Hb with conversion of Fe^{2+} to Fe^{3+}.

The high sensitivity of magnetic capture, which exceeds the sensitivity of the spectrophotometric methods for measurements on solutions, allows one to study the stability of erythrocytes over time and under different conditions of functioning. Thus, in the incubation of erythrocytes for three hours in a buffer with pH from 6.0 to 9.5 at 20 °C it was shown that the change in susceptibility of the cells corresponds to accumulation in them of less than 1% metHb over this time.

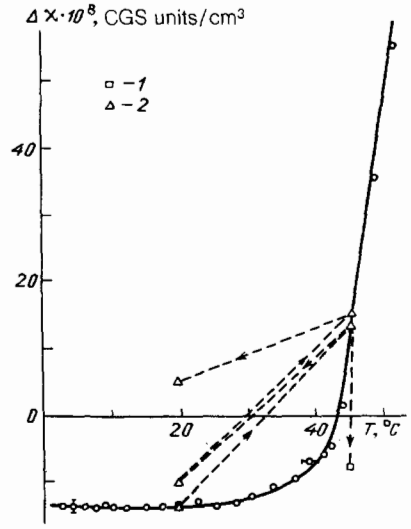

FIG. 12. Temperature dependence of the magnetic susceptibility of intracellular oxyHb (pH ~ 7.4). *1*–variation of the susceptibility after bubbling with oxygen for 30 min at 45 °C; *2*–variation of the susceptibility upon changing the temperature in the directions indicated by the arrows.[38]

3.2. Oxygen-exchange processes in erythrocytes

One can study by the magnetic-capture method oxygen-exchange processes in individual cells by measuring their magnetophoretic mobility as a function of the partial pressure of oxygen in the suspension. The dependence of the susceptibility of individual erythrocytes relative to the buffer on the time of diffusion of oxygen through a gas-permeable membrane as argon is blown around the measurement cell is shown in Fig. 13 (pH = 7.4; 25 °C). The same diagram shows the dependence of the susceptibility of the cells on the time of diffusion of oxygen into the suspension as air is blown around the cell $P_{O_2} = 150$ Torr). The shown dependences characterize the change in the magnetic susceptibility of individual cells upon dissociation and binding of oxygen to the intracellular hemoglobin. We see from the diagram that deoxygenation of the suspension for ~ 1 hour leads to "saturation" of the susceptibility, at which the intracellular hemoglobin is fully deoxygenated. A triply repeated dissociation-binding of a given suspension yields identical susceptibility results within the limits of error, which indicates the absence of irreversible changes, in particular, methemoglobinization.

The degree of saturation with oxygen of the intracellular Hb (Y) is connected to the magnetic susceptibility χ of the erythrocyte relative to the buffer, under the condition of additive contribution to the susceptibility of oxy- and deoxyhemoglobin, by the relationship

$$Y = \frac{\chi - \chi^{\text{deoxy Hb}}}{\chi^{\text{oxy Hb}} - \chi^{\text{deoxy Hb}}}, \tag{11}$$

Here χ^{oxyHb} and χ^{deoxyHb} are the magnetic susceptibilities relative to the buffer of completely oxygenated and deoxygenated cells. Upon using the experimentally determinable dependence of the concentration of dissolved oxygen in the region of magnetic capture on the time of gas exchange and the dependence in Fig. 13, one can construct a Hill graph (see Fig. 14) for the oxygenation and deoxygenation of intracellular Hb. Since the time of magnetic-capture measurements is ~ 10 s, while the time of binding (and release) of oxygen with heme is ~ 50 ms,[39] the dependences in Fig. 13

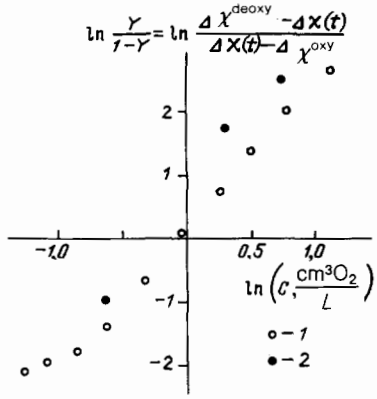

FIG. 14. Hill graph for dissociation (*1*) and binding (*2*) of intracellular hemoglobin with oxygen (25 °C, ph ~ 7.4).

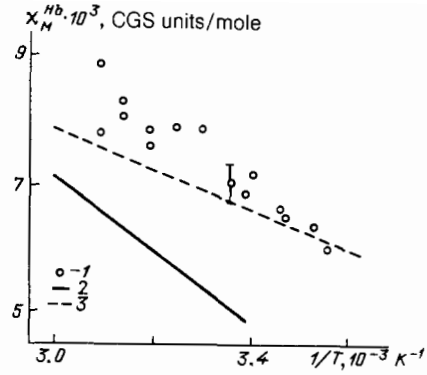

FIG. 15. Temperature dependence of the molar magnetic susceptibility of nitrite methemoglobin. *1*–intracellular; *2*–in solution;[41] *3*–calculated dependence according to Eqs. (12) and (13) for $\Delta H = 5.9$ kcal/mole and $\Delta S =$ kcal·deg/mole.

are of equilibrium type. We see from the data presented in Fig. 14 that the oxygen affinity P_{50} of intracellular Hb (the partial pressure of oxygen at which 50% of the binding regions are saturated) and the Hill cooperativity parameter n (which characterized the steepness at $Y = 0.5$) upon decreasing the partial pressure of oxygen in the suspension ($n = 1.4$; $P_{50} = 0.68$ cm^3 O_2/L differ from n and P_{50} upon increasing the oxygen pressure ($n = 2.8$; $P_{50} = 0.45$ cm^3 O_2/L). The noted irreversibility of the dissociation and binding curves perhaps is due to a change in the permeability of the erythrocyte membrane in oxygen exchange.[40]

3.3. The magnetic susceptibility of intracellular methemoglobin

For certain Fe^{3+} complexes of hemoglobin the difference in energies of the high- and low-spin states at room temperature is so small that mutual equilibrium transitions can become possible between them. Magnetic-susceptibility measurements have shown that the Fe^{3+} ion has an effective moment of $4.5\,\mu_B$ at pH ~ 9.5 and $5.8\,\mu_B$ at pH ~ 7.0. These values are intermediate between those found for high-spin Fe^{3+} in HbF ($5.9\,\mu_B$) and low-spin in HbCN (2.3–2.5 μ_B).[41]

Analysis of the temperature dependence of the magnetic susceptibility of the Fe^{3+} ion in the quaternary R- and T-structures[6)] between 300 and 90 K showed[41] that at low temperatures (90–250 K) the susceptibility varies according to the Curie law and the Fe^{3+} ion remains in the low-spin state. In the region 200–250 K appreciable deviations were observed from the Curie law that reflect the shift of equilibrium toward formation of high-spin states. At all temperatures the magnetic moment in the T structure was higher than in the R structure. At 0–30 °C the magnetic susceptibility reflects the existence of spin equilibrium depending on the temperature and can be represented in the form

$$\chi = \frac{1}{8T}\,\frac{k\mu_H^2 + \mu_L^2}{k+1}, \qquad (12)$$

Here k is the equilibrium constant between the high- and low-spin states, and μ_H and μ_L are respectively the magnetic moments of these states. Adjustment of the experimental data yields the best agreement for χ according to (12) expressed in terms of the Gibbs energy (ΔG):

$$k = \exp\left(-\frac{\Delta G}{RT}\right) = \exp\left(-\frac{\Delta H - T\Delta S}{RT}\right) \qquad (13)$$

with empirically selected values of ΔH and ΔS.

Figure 15 shows the temperature dependence of the molar magnetic susceptibility of intracellular nitrite metHb obtained by magnetic capture of individual erythrocytes. For comparison, the results are presented there of measurements of χ_M obtained in solutions of nitrite-metHb,[41] which are satisfactorily described by (12) and (13) with calibration values of the enthalpy $\Delta H = 2.6$ kcal/mole and of the entropy $\Delta S = 5.7$ kcal·degree/mole. As we see, the susceptibility of nitrite metHb has the same slope as the susceptibility of the solution, but exceeds it somewhat in absolute values. An attempt to describe the behavior of intracellular metHb with Eqs. (12) and (13) yielded best agreement for $\Delta H = 5.9$ kcal/mole, $\Delta S = 15$ kcal·degree/mol (dashed line through the experimental points), but with a slope smaller than the experimental. The mentioned quantitative disagreements between the behavior of $\chi(T)$ of nitrite metHb in solutions and in cells can arise from the extremely high sensitivity of Hb to the action of oxidizing agents,[7)] which alter the spin state of the heme iron:[26] the high-spin state predominates in bound Fe-ONO, and the low-spin state in Fe-NO_2. Apparently in cells the equilibrium shifts toward the low-spin states with increasing temperature. The spin equilibrium of nitrite metHb in cells is also observed upon titration. Figure 16 shows the pH dependence of the magnetic susceptibility of erythrocytes containing nitrite-metHb relative to the buffer at 20°, as obtained by the magnetic-capture method. The increase in susceptibility upon protonation involves stabilization of the high-spin T form.

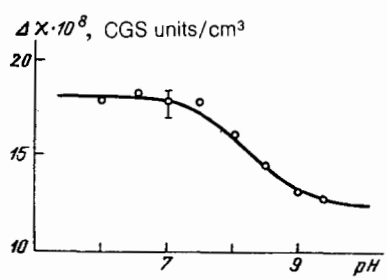

FIG. 16. Magnetic susceptibility of erythrocytes containing nitrite methemoglobin relative to the buffer for different pH values (20 °C).

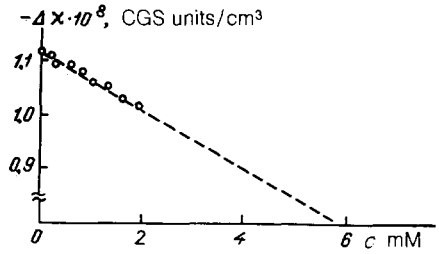

FIG. 17. Relative magnetic susceptibility of oxygenated erythrocytes as a function of the concentration of oxyhemoglobin in the buffer medium.

3.4. Use of erythrocytes as test objects

One measures by the magnetic-capture method the susceptibility of a particle relative to the susceptibility of the buffer, which is assumed to be known. The converse can happen: measurement of the susceptibility of the medium by capture of a particle with known susceptibility. Thus, in Ref. 42 the susceptibility of blood plasma was measured in this way, with a bubble of hydrogen used as the test object. As a test object with known magnetic and hydrodynamic characteristics, one can also use erythrocytes. Figure 17 shows the dependence of the magnetic susceptibility of oxygenated erythrocytes relative to the buffer when containing varying concentrations of oxyHb ($c_{\rm buf}^{\rm Hb}$). The measurements were performed up to a concentration below 2 mM, since a change in the cell shape was observed at higher concentrations. We find from (5) under the assumption of additive contributions that the susceptibility of the cell relative to the buffer is

$$\chi = (c_{\rm c}^{\rm Hb} - c_{\rm буф}^{\rm Hb})\,(\chi_{\rm Hb} - \chi_{\rm буф}). \qquad (14)$$

The point of intersection of the extrapolated dependence with the axis of abscissas corresponds to the concentration of hemoglobin in the cell, while the tangent of the slope angle corresponds to the magnitude of the magnetic susceptibility of the oxy form of Hb.

4. MAGNETIC PROPERTIES OF BILAYER LIPID MEMBRANES

4.1. Magnetic susceptibility of a lipid bilayer

In a lipid-water system at low lipid concentration multilayer spherical or cylindrical aggregates–liposomes–can form spontaneously (Fig. 18). Each bilayer film amounts to two Gibbs monolayers of amphiphiles with oleophilic "tails" in the form of one or two hydrocarbon chains turned toward one another.[43] The thickness of a bilayer is ~50 Å. Such a bilayer film amounts to the simplest artificially created supermolecular structure, and is a model of the core of a biological membrane. Up to now there has been very sparse information on the magnetic properties of such films.[1,2] In measuring the magnetic susceptibility of a suspension of liposomes, one must distinguish the membrane component proper of the susceptibility from the overall signal, in which the lipid component amounts to a quantity of the order of a percent or several percent if the lipid exists in a lamellar phase. In all probability this is precisely why the known studies have been performed at a single temperature–room temperature.

The high sensitivity of magnetic capture has enabled performing measurements of the capture parameters of single multilayer spherical liposomes of a natural lipid–egg lecithin (EL) and estimating the magnetic susceptibility of a bilayer made of this lipid.[44] Subsequently the number of lipids studied in this way has been supplemented with a synthetic phospholipid–dipalmitoyl lecithin (DPL) and a natural one–erythrocyte-membrane lipid (EML).[45,46] The compensative character of the measurements in magnetic capture enables determining the susceptibility directly of the membrane component of the vesicle, which depends on the magnetic moments of the lipids forming the bilayer, their mutual arrangement, the interaction with one another within the bilayer, between the layers, and with the water surrounding them. An aqueous suspension of liposomes contains vesicles of varying dimension (radius ~3–4 μm) with varying numbers of concentric bilayers. The density of the lipids is close to that of water. The lipid vesicles practically do not sediment, which substantially complicates the determination of the magnitudes of their effective Stokes radii–$R_{\rm eff}$. Therefore, in calculating the magnetic susceptibility of a spherical liposome with respect to the buffer from its magnetic-capture data according to (5), the value of $R_{\rm eff}$ of a liposome has been assumed equal to the value of its geometric radius, which was determined by measuring the radius on a monitor screen (Fig. 19).

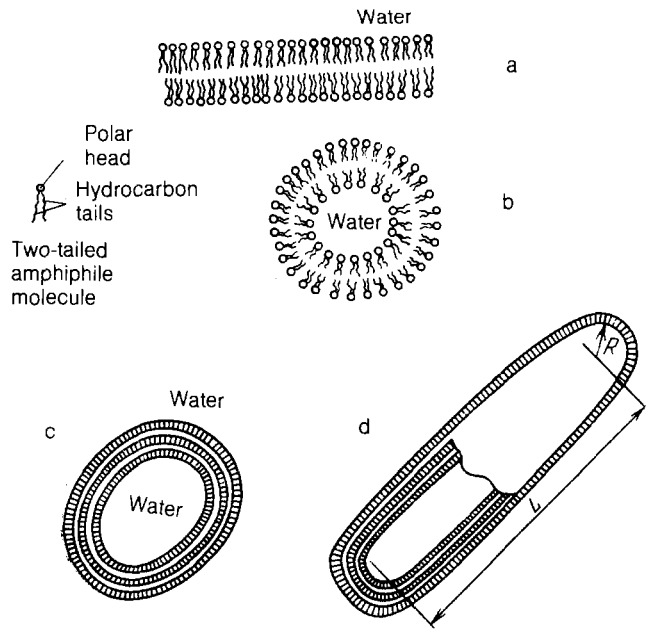

FIG. 18. Schematic drawing of bilayer aggregates formed by phospholipids in aqueous media: a–fragment of a lamellar structure; b–single-layer, and c–multilayer spherical liposomes; d–multilayer cylindrical vesicle. The shape parameters of the cylindrical vesicle subject to measurement are shown.

The magnetic susceptibility χ_i of the ith liposome relative to the buffer involves the susceptibility of the medium $\chi_{\rm buf}$ and of the lipid $\chi_{\rm l}$ by the evident relationship

$$\chi_i = (\chi_{\rm l} - \chi_{\rm buf})\,\frac{v_i}{V_i}, \qquad (15)$$

Here V_i is the volume of the measured ith vesicle, and v_i is the volume of the lipid component in it. Upon assuming that the liposome consists of an integral number n of concentric bilayers of identical thickness l, with $nl \ll R_i$,[8)] we find that the product for each ith liposome is proportional to the number of bilayers n_i in it. That is, we have

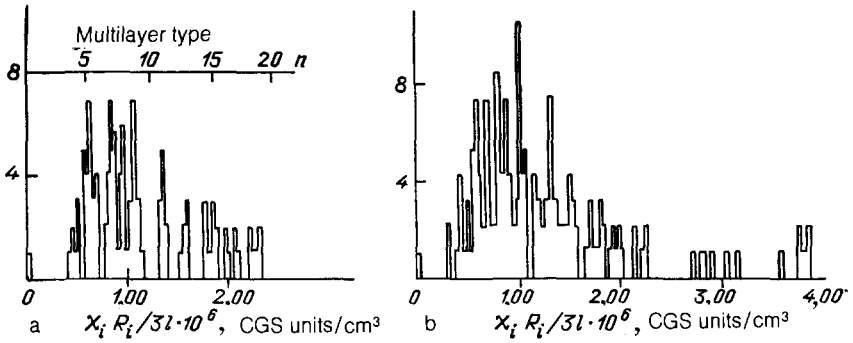

FIG. 19. Typical histograms of the distribution of liposomes of EL (a) and DPL (b) with respect to values of $\chi R_i/3e$.[45]

$$\chi_i \frac{R_i}{3e} = n_i(\chi_l - \chi_{\text{buf}}). \tag{16}$$

The proportionality coefficient equals the magnetic susceptibility of the bilayer packing of lipid molecules relative to the buffer medium. Thus the experimentally determinable values of $\chi_i R_i/3l$ of the vesicles being studied must coincide with the sequence of discrete values $n_i(\chi_l - \chi_{\text{buf}})$ for integral values of n_i.

Figure 19 shows typical histograms of the distribution of liposomes made of EL and DPL with respect to their values of $\chi_i R_i/3e$. We see several maxima in each histogram. Processing of the results of measurements of the values of $\chi_i R_i/3e$ of a large number of liposomes enabled finding mean values of the proportionality coefficients $(\chi_l - \chi_{\text{buf}})$ such that the product $(\chi_l - \chi_{\text{buf}})$ best coincided for integral n_i with the maxima on the histograms. Precisely these integral values were treated as the lamellarity, i.e., as the number of concentric bilayers in the measured liposomes, while the proportionality coefficient $(\chi_l - \chi_{\text{buf}})$ was treated as the relative susceptibility per unit volume of the bilayer packing of lipid molecules.

The histograms lack data on the distribution of liposomes with a small number of bilayers. Slowly moving vesicles were also observed in the experiments. However, the time of magnetic capture of such particles is determined with great error, and hence their susceptibility was not determined. The absence of maxima corresponding to a large number of bilayers is due to both defects, the number of which increases with increase in the lipid content in the liposome (breakdown of concentric packing, inclusion of dry lipid matter, etc.), and to breakdown of the condition $n_i l \ll R_i$.

Figure 20 presents the magnetic susceptibilities of bilayers of DPL, EML, and EL measured in this way as functions of the temperature. Each point in these dependences is the result of processing the corresponding histogram of the distribution of the vesicles being studied with respect to the value of $\chi_i R_i/3l$. Here, in determining χ_i by (5), account was taken of the variation with temperature of the viscous properties of the medium but not the variation of its magnetic properties, so that each value of $\chi(T)$ shown in Fig. 20 was obtained with allowance for the susceptibility of the medium, which was assumed not to depend on the temperature, and to equal the susceptibility of pure water.

As we see from Fig. 20a, with decreasing temperature one observes a temperature-independent behavior of χ_{DPL} down to the temperature of the main transition from the liquid-crystalline state to the gel phase at $T_c \sim 41$ °C. Here one observes a sign change of the magnetic capture–below T_c the liposomes became more diamagnetic than the buffer, and moved toward the filament into the region of least magnetic field around it. Below T_c the susceptibility proved to be close to that of DPL in the crystalline state.[47] According to Ref. 48, upon solidification the bilayer of DPL undergoes a

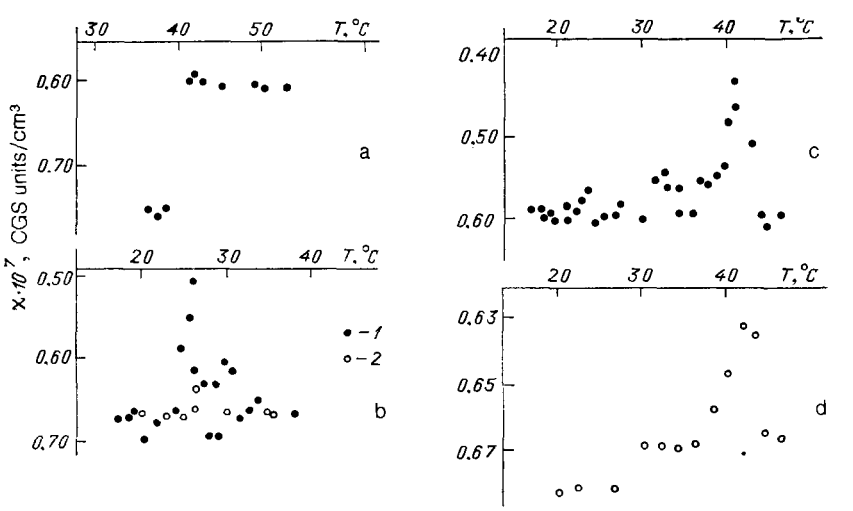

FIG. 20. Temperature dependences of the magnetic susceptibility of bilayers. a–DPL; b–EML (*1*–on heating; *2*–on cooling the suspension). c–EL, as obtained by the magnetic-capture method. d–The same for a 15% suspension of EL obtained by measurement in a magnetic balance. The cases of Fig. c and d were obtained upon heating.

transition to the P_β phase, accompanied by a change in the molecular volume by about 7%. Yet the observed change in the susceptibility of DPL in this transition (see Fig. 20a) is substantially larger and cannot be explained alone by the change in the molecular volume, as was assumed in Ref. 49, where the data on χ_{DPL} (T) obtained by SQUID magnetometry are given in relative units.

The behavior is interesting of $\chi(T)$ of bilayers of EML and EL existing in the liquid-crystalline state and obtained upon raising the temperature of the suspension (see Fig. 20b,c). The temperature dependences of the susceptibility of the two natural bilayers have similar, sharply marked features, unusual in form, at certain temperatures characteristic of each of them. In studying the susceptibility of EML in cooling from 40 °C, the features noted upon heating were not observed. Unfortunately the restoration of the values of χ_{EML} with time was not studied.

At present it is difficult to measure in any other way the susceptibility of a lipid bilayer from measurements of an aqueous suspension of liposomes containing less than 1% lipid. Starting with the magnitude of the feature in $\chi(T)$ in EL at ~41 °C, one can expect resolution of this feature upon studying a 15% aqueous suspension of EL with a highly-sensitive Faraday magnetic balance. Studies were performed on such a suspension, in which EL was assumed to exist in a disordered lamellar phase. The results of these studies are shown in Fig. 20d. As we see, in the region of 30 °C one observes a small change in the susceptibility, which correlates with the change in $\chi(T)$ obtained by the magnetic-capture method. In the region of 40 °C we observe a feature similar to that obtained by using magnetic capture, on either side of which we also do not observe an appreciable difference in the values of χ. The measurements using a balance showed that in EL, just as in EML, there is a temperature irreversibility in $\chi(T)$–no feature was observed upon lowering the temperature from 45 °C.

4.2. Magnetic capture of cylindrical liposomes and the anisotropy of the magnetic susceptibility of the lipid bilayer

A method was proposed in Ref. 50 for determining the anisotropy of the magnetic susceptibility of a bilayer in the L_α phase. The magnitude of the difference between the longitudinal $\chi_\parallel$ (along the director) and the transverse $\chi_\perp$ (perpendicular to the director) of the components of the susceptibility tensor was determined from the condition of equality of the magnetic moment to the mechanical moment upon rotation of cylindrical liposomes in the homogeneous magnetic field H_0:

$$(\chi_\parallel - \chi_\perp)\,\delta_i = \frac{kT\,(\ln \operatorname{tg}\theta_0 - \ln \operatorname{tg}\theta_t)}{L_i R_i D_k H_0^2 t}\,; \qquad (17)$$

Here $\delta_i = \ln_i$ is the thickness of the lipid layer of the liposome, θ_0 and θ_i are the angles between the direction of the field and the long axis of the cylinder at the instant of turning on the field and after the time t, respectively, D_k is the rotational diffusion coefficient, L_i is the length of the cylindrical part, and R_i is the radius of the hemisphere closing the cylinder.

Magnetic capture of cylindrical vesicles enables one to determine in the same way the magnitude of the anisotropy of a lipid bilayer $\chi_\parallel - \chi_\perp$.

The process of capture of a cylindrical vesicle starts with the phase of its rotation in the field, which occurs far faster than the capture proper of the particle by the filament. Measurement of the parameters of the rotation and capture of such a particle enables one not only to determine the value of the diamagnetic anisotropy $\chi_\parallel - \chi_\perp$ of the bilayer, but also to simplify this procedure considerably, owing to the possibility of independent determination of the lamellarity: the number n_i of bilayers is determined from the value of the susceptibility of the cylindrical liposome measured and the susceptibility of a bilayer as obtained in advance from measurements on spherical vesicles. Then by using (17) and the experimentally determined quantities θ_0, θ_i, D_k, L_i, R_i, and t, one calculates the value of the difference $\chi_\parallel - \chi_\perp$. Both methods: the magnetic capture of cylindrical vesicles and their rotation in a homogeneous magnetic field yield the same result within the limits of error of the measurements. Figure 21 shows the results of measuring the temperature dependence of $\chi_\parallel - \chi_\perp$ of a bilayer of EL as obtained by both methods. As we see, this relationship has features at the same temperatures as does $\chi_{EL}(T)$. One can estimate from the data of independent measurements of the diamagnetic anisotropy $\chi_\parallel - \chi_\perp$ and the magnetic susceptibility χ of a bilayer, which for spherical vesicles is $(\chi_\parallel + 2\chi_\perp)/3$, the components of the diamagnetic-susceptibility tensor of a bilayer of lipid molecules. Thus, for EL, the components of the tensor χ obtained from the data of Figs. 20c and 21 are given in Fig. 22. We can see that the region of the features manifests a simultaneous decline in both components $\chi_\parallel$ and $\chi_\perp$, with $\chi_\perp$ declining more strongly. We note that the compo-

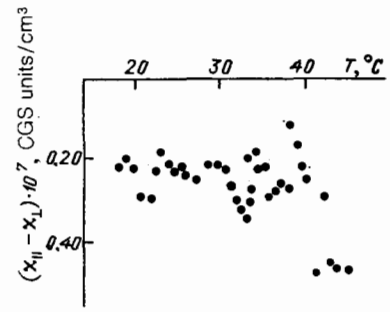

FIG. 21. Temperature dependences of the anisotropy of magnetic susceptibility $(\chi_\parallel - \chi_\perp)$ of a bilayer of EL obtained upon heating the suspension.

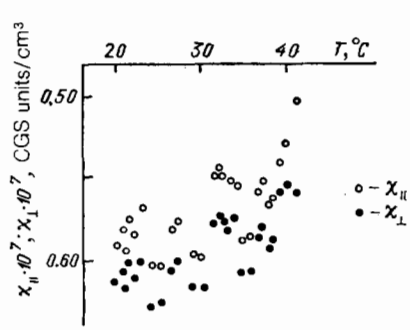

FIG. 22. Calculated values of the longitudinal $\chi_\parallel$ and transverse $\chi_\perp$ components of the magnetic-susceptibility tensor of a bilayer of EL as functions of the temperature.

nents of the tensor χ in lipid systems have been determined only for crystals of DPL at room temperature[47] from the rotation of microcrystallites in a homogeneous field and from measurements of its mean susceptibility in a vibrating magnetometer.

CONCLUSION

Magnetic capture belongs to the few methods that enable gaining information, without violating their integrity, on a single functioning cell and on an artificially created aggregate that models the cell membrane. The high sensitivity and universality–the possibility of measuring both diamagnetic and paramagnetic induced moments, as well as the relative simplicity of the interpretation of the translational displacement of a microparticle during its magnetic capture, favorably distinguish this method of study. However, despite a certain uniqueness, magnetic capture for a long time did not find its due practical application. This mainly involved not only the lack of ready-made laboratory instrumentation or of some of its components requiring jeweler's precision, but also in many ways was determined by the lack of the needed recording and computing technique capable of substantially simplifying the measurement process. Precisely the appearance of such a reliable videorecording technique having the necessary resolution and of sufficiently powerful computers with television data input can give a strong impetus toward the widespread use of magnetic capture. We note some fundamental lines, as we see them, for such studies.

First there are the studies of the individual magnetic properties of cells, to be conducted also with the goal of identifying their physiological states, and directed toward diagnostics and magnetic separation. Here is presented a broad set of studies of the metabolism of cells, the influence on their functioning of external agents and various types of ligands artificially introduced into the buffer medium. Thus we can already mention the possibility of magnetophoretic measurement of the kinetics of enzymatic reduction of methemoglobin in individual erythrocytes and magnetic screening for heterozygote carriers of an enzyme deficiency.[51] Especially promising in our opinion are studies of the magnetic screening of immunological binding of antibodies, proteins, or virus particles without previous chemical modification of them. The results obtained in our laboratory of the studies begun along this line of studies allow us to hope for creation of a new type of immunodiagnostics favorably distinguished from the widely applied radioisotope, immunoenzyme, and immunofluorescence methods.

Studies of the magnetic properties of liposomes–bilayer aggregates that model the cell membrane–is another, quite new application of magnetic capture. As yet not all is irreproachable from the standpoint of "purity" of experimentation. A subtle point is the magnitude of the Stokes resistance, which was considered in the examples discussed above to be invariant, and was determined from the geometric dimensions of the vesicles. As we see from the example of erythrocytes, processes that occur inside the membrane can alter the value of R_{eff} of the cell. This can happen, e.g., owing to a change in the area per molecule in the bilayer (this is indicated by the change in the components of the χ tensor observable in EL). In turn, this can alter the state of the near-surface layer of the model aggregate or cell owing to a change in various types of binding constants. In the case of erythrocytes containing oxyHb (see Fig. 12), the temperature features of the magnetic-capture times, in determining the susceptibility of a cell by using Eq. (5), are compensated by the features of the values of R_{eff} observed at the same temperatures. As a whole, they weaken the temperature-independent susceptibility of the entire cell. A knowledge of the concrete values of the effective radii of liposomes, whose measurement seems to be a quite solvable problem, can either weaken or strengthen the observed features of $\chi(T)$ of a lipid bilayer.

Omitting a discussion of the results of studies of the magnetic properties of bilayer lipid films as extending beyond the scope of this article, we note that the features in $\chi(T)$ observed in bilayers of EL and EML are explicitly nonequilibrium in type, resembling more some dissipative structures than structural phase transitions, as they are commonly termed at present.[52] Perhaps magnetic capture is the only possible method of studying the magnetic properties of liposomes arising in an aqueous medium at concentrations of lipid less than a percent. We can hope that we can obtain new data based on these studies that will draw us closer to an understanding of the nature of both the observed features and of the lipid-lipid and lipid-protein interactions that determine the structure and properties of the cell membrane.

[1)] Such widely known methods as the magnetic balance, EPR, or SQUID magnetometry possess at least two orders of magnitude lower sensitivity with respect to magnetic moment.

[2)] The possibility of diamagnetic capture and of determination of the magnetic susceptibility of small particles from the character of their motion in a liquid medium near the surface of a magnetized cylinder was pointed out in Ref. 6. Ink the same place an experimental measurement was made of the field distribution near a magnetized cylinder (from the action of the force on a suspended bismuth particle), a graphical solution of Eq. (1) was presented, a proposal was made on the possibility of diamagnetic capture, and paramagnetic capture of polystyrene particles 25–50 μm in diameter by a transversely magnetized rod was observed.

[3)] One uses a different scheme of capture for repeated measurements of the magnetic capture of a given cell (see also Fig. 9).

[4)] Information on the content of methemoglobin in healthy erythrocytes and its variations in pathology within the range 0.3–2.0% appears to be very important.[16] The known spectrophotometric methods of determining methemoglobin enable one to detect the presence of methemoglobin in cells at the level of 0.8–1.0%, but it is necessary to release the contents of the cell and remove the membranes.

[5)] One can find information on erythrocytes and on the structure and functions of Hb, e.g., in Ref. 25.

[6)] The two different conformational states of the Hb molecule are T–tense, and R–relaxed, which differ in the degree of affinity for oxygen.

[7)] A 23-mM solution of $NaNo_2$ was used as the oxidizer. The presence of the met form was monitored by the absorption spectra of hemolysates and amounted to 97–99%.

[8)] The thickness of a bilayer is ~ 40 Å,[43] so that this condition is easily fulfilled for vesicles of radius $\sim 4\ \mu$m and $n \sim 10$.

[1] A. A. Vedenov and E. B. Levchenko, Usp. Fiz. Nauk **141**, 3 (1983) [Sov. Phys. Usp. **26**, 747 (1983)].

[2] A. S. Sonin, Usp. Fiz. Nauk **153**, 273 (1987) [Sov. Phys. Usp. **30**, 875 (1987)].

[3] *Biophysical Effects of Steady Magnetic Fields: Proceedings of the Workshop*, Les Houches, France, Springer-Verlag, Berlin, 1987.

[4] J. H. P. Watson, J. Appl. Phys. **44**, 4209 (1973).

[5] S. Uchiama, S. Kondo, M. Takayasu, and I. Eguchi, IEEE Trans. Magn. **MAG-12**, 895 (1976).

[6] S. J. Gill and C. P. Malone, Rev. Sci. Instrum. **34**, 788 (1963).

[7] R. R. Birss and M. R. Parker, IEEE Trans. Magn. **MAG-15**, 1523 (1979).

[8] C. G. Caro *et al.*, *The Mechanics of the Circulation*, Oxford University Press, 1978 (Russ. transl., Mir, M., 1981).

[9]E. I. Kondorskiĭ, S. B. Norina, and A. N. Shalygin, Biofizika **25**, 353 (1980) [Biophysics (USSR) **25**, 367 (1980)].
[10]E. I. Kondorskiĭ, S. B. Norina, N. V. Litvinchuk, and A. N. Shalygin, *ibid.* **26**, 1104 (1981) [Biophysics (USSR) **26**, 1127 (1981)].
[11]F. Paul, D. Melville, and S. Roath, IEEE Trans. Magn. **MAG-18**, 792 (1982).
[12]Yu. A. Plyavin' and É. Ya. Blum, Magn. Gidrodinamika, No. 4, 3 (1983) [Magnetohydrodynamics (USA) **19**, 349 (1983)].
[13]A. N. Shalygin, S. B. Norina, and E. I. Kondorskiĭ, Biofizika **29**, 845 (1984) [Biophysics (USSR) **29**, 922 (1984)].
[14]A. N. Shalygin, S. B. Norina, and E. I. Kondorsky, J. Magn. Magn. Mater. **31-33**, 555 (1983).
[15]J. Happel and H. Brenner, *Low Reynolds Number Hydrodynamics*, Prentice-Hall, Englewood Cliffs, N. J., 1965 (Russ. Transl., Mir, M., 1976, p. 630).
[16]M. S. Kushakovkiĭ, Clinical Forms of Damage of Hemoglobin (in Russian), Meditsina, L., 1968, p. 325.
[17]A. N. Shalygin, S. B. Norina, V. B. Ginzburg, A. M. Chekaev, and S. V. Rykov, Authors' Ceritificate No. 1198431; Byul. Izobreteniĭ SSSR No. 46, 172 (1985).
[18]Yu. A. Plyavin', É. Ya. Blum, L. I. Yavorkovskiĭ, I. T. Medne, and R. Ya. Ozols, Magn. Gidrodinamika, No. 1, 140 (1979) [Magnetohydrodynamics (USA) **15**, 115 (1979)].
[19]F. J. Friedlaender, M. Takayasu, T. Nakano, and D. R. Kelland, J. Magn. Magn. Mater. **15–18**, 1555 (1980).
[20]V. A. Miroshnikov and R. Ya. Ozols, Magn. Gidrodinamika, No. 4, 5 (1982) [Magnetohydrodynamnics (USA) (1982)].
[21]D. Melville, F. Paul, and S. Roath, Nature **255**, 706 (1975).
[22]C. S. Owen, Biophys. J. **22**, 171 (1978).
[23]M. D. Graham, J. Appl. Phys. **52**, 2578 (1981).
[24]C. S. Owen, *ibid.* **53**, 3884 (1982).
[25]M. A. Fedorov, ed., *Normal Hemopoiesis and Its Regulation* [in Russian], Meditsina, M., 1976.
[26]M. F. Perutz, Ann. Rev. Biochem. **48**, 327 (1979).
[27]L. Pauling and C. D. Coryell, Proc. Natl. Acad. Sci. U.S.A. **22**, 210 (1936).
[28]L. Pauling, Nature **203**, 182 (1964).
[29]J. S. Griffith, Proc. R. Soc. London A **235**, 23 (1956).
[30]J. B. Wittenberg, B. A. Wittenberg, J. Peisach, and W. E. Blumberg, Proc. Natl. Acad. Sci. U.S.A. **67**, 1846 (1970).
[31]M. Bacci, M. Cerdonio, and S. Vitale, Biophys. Chem. **10**, 113 (1979).
[32]M. Cerdonio, S. Morante, D. Torresani, S. Vitale, A. de Young, and R. W. Noble, Proc. Natl. Acad. Sci. U.S.A. **82**, 102 (1985).
[33]J. S. Philo, U. Dreyer, and T. M. Schuster, Biochemistry **23**, 865 (1984).
[34]S. P. Savicki, G. Lang, and M. Ikeda-Saito, Proc. Natl. Acad. Sci. U.S.A. **81**, 5417 (1984).
[35]L. A. Piruzyan, A. A. Kuznetsov, V. M. Chikov, and I. T. Plotnikova, Izv. Akad. Nauk SSSR Ser. Biol., No. 6, 894 (1984) [Biol. Bull. Acad. Sci. USSR (1984)].
[36]E. A. Chernitskiĭ and A. V. Vorobeĭ, *Structure and Function of Erythrocyte Membranes* [in Russian], Nauka i Tekhnika, Minsk, 1981, p. 216.
[37]É. Ya. Blum, R. Ya. Ozols, and Yu. A. Plyavin'sh, Izv. Akad. Nauk Latv. SSR, No. 1, 127 (1987).
[38]A. N. Shalygin and K. A. Krotov, Biofizika **33**, 529 (1988) [Biophysics (USSR) **33**, 568 (1988)].
[39]K. D. Vandegriff and J. S. Olson, J. Biol. Chem. **259**, 1269 (1984).
[40]M. V. Fok, A. R. Zaritskiĭ, and G. A. Prokopenko, Biofizika **33**, 622 (1988) [Biophysics (USSR) **33**, 667 (1988)].
[41]C. Messana, M. Cerdonio, P. Chenkin, P. W. Noble, G. Fermi, P. N. Perutz, and M. F. Perutz, Biochemistry **17**, 3652 (1978).
[42]M. Takayasu, N. Duske, S. R. Ash, and F. J. Friedlaender, IEEE Trans. Magn. **MAG-18**, 1520 (1982).
[43]W. H. De Jeu, *Physical Properties of Liquid Crystalline Materials*, Gordon and Breach, New York, 1980 (Russ. Transl., Mir, M., 1982).
[44]A. N. Shalygin, T. V. Vyshenskaya, and E. V. Perevedentseva, Biofizika **32**, 683 (1987) [Biophysics (USSR) **32**, 737 (1987)].
[45]A. N. Shalygin, E. V. Perevedentseva, and T. V. Tyazhelova, Zh. Fiz. Kim. **64**, 1337 (1990) [Russ. J. Phys.Chem. (1990)].
[46]A. N. Shalygin, E. V. Perevedentseva, and M. A. Baryshev, *ibid.*, p. 1623 [Russ. J. Phys. Chem. (1990)].
[47]Y. Kamamura, I. Sakurai, A. Ikegami, and S. Iwayanagi, Mol. Cryst. Liq. Cryst. **61**, 77 (1981).
[48]D. M. Small, ed., *Handbook of Lipid Research: The Physical Chemistry of Lipids*, Plenum Press, New York, 1986, p. 487.
[49]R. K. Kunze, Jr., J. T. Ho, and E. P. Day, Biophys. J. **30**, 359 (1980).
[50]E. Boroske and W. Helfrich, Biophys. J. **24**, 863 (1976).,
[51]A. N. Terent'ev, *Abstract of Candidate's Dissertation in Chemical Sciences* [In Russian], Institute of Physical Chemistry of the Academy of Sciences of the USSR, Moscow, 1989.
[52]V. G. Ivkov and G. N. Berestovskiĭ, *The Lipid Bilayer of Biological Membranes* [in Russian], Nauka, M., 1982.

Translated by M. V. King